

# Uncovering the Structure of Human Red Hair Pheomelanin: Benzothiazolythiazinodihydroisoquinolines As Key Building Blocks

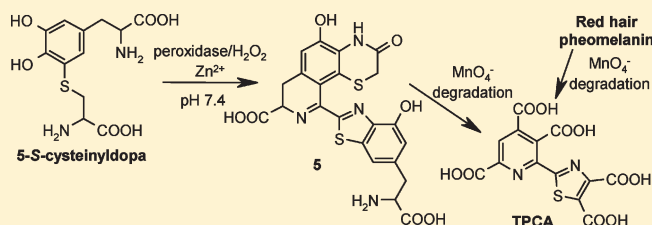
Giorgia Greco,<sup>†</sup> Lucia Panzella,<sup>†</sup> Luisella Verotta,<sup>‡</sup> Marco d'Ischia,<sup>†</sup> and Alessandra Napolitano<sup>\*,†</sup>

<sup>†</sup>Department of Organic Chemistry and Biochemistry, University of Naples Federico II, Via Cintia 4, I-80126 Naples, Italy

<sup>‡</sup>Department of Organic and Industrial Chemistry, Via Venezian 21, I-20133 Milan, Italy

**S** Supporting Information

**ABSTRACT:** Biomimetic oxidation of the pheomelanin precursor 5-*S*-cysteinyl-dopa in the presence of Zn<sup>2+</sup> ions led to the isolation of two isomeric products, one of which could be identified as the benzothiazolythiazinodihydroisoquinoline **5**, while the other proved too unstable for a complete characterization. Both these products were converted into more stable oxidized forms, which after ethylchloroformate derivatization were characterized as the ethyl ester/ethoxycarbonyl isoquinolines **8** and **9**. Compound **5** exhibited absorption characteristics similar to those of red hair pheomelanin, including a main band around 400 nm in acids. Similarly to red hair pheomelanin and synthetic pigments, **5** afforded on chemical degradation a thiazolylpyridinecarboxylic acid fragment. Model chemical studies allowed the proposal of a formation mechanism for the benzothiazole and dihydroisoquinoline systems in compound **5**.



Pheomelanins are a reddish-brown, sulfur-containing subgroup of melanin pigments typically found in mammalian hair and chicken feathers.<sup>1–3</sup> Interest in these pigments stems from their association with the familiar red hair phenotype of Celtic origin (the red hair color RHC phenotype, the “redheads”) characterized by a fair complexion, extensive freckling, and high susceptibility to sunburn and skin cancer, including melanoma.<sup>4–6</sup> The existence of a possible causal relationship between pheomelanins and UV susceptibility is the subject of a long-lasting debate.<sup>7</sup>

A definitive assessment of the actual role of pheomelanin in UV susceptibility and actinic damage awaits, however, complete elucidation of the fundamental molecular components of these heterogeneous and elusive biopolymers,<sup>8,9</sup> as well as an understanding of their biosynthetic origin and structural organization within the subcellular organelles, the melanosomes.<sup>10,11</sup> Defining the basic structural motifs of human red hair pheomelanin is of the utmost importance in the prospects of determining what chromophores activate molecular oxygen and mediate photo-toxic reactions in cellular systems.<sup>12–14</sup>

Like the more widespread black eumelanins found in dark skinned individuals, pheomelanins are produced by tyrosinase-catalyzed oxidation of tyrosine leading to dopaquinone. Their formation, however, is the result of a metabolic switch of the eumelanin pathway, which is sustained by elevated levels of cysteine (>1 μM)<sup>15</sup> (Figure 1). Chemically, the process is initiated by the reaction of dopaquinone with cysteine, leading to 5-*S*-cysteinyl-dopa (**1**) (74%) as the main product, with 2-*S*-cysteinyl-dopa in much smaller amounts, and other minor isomers.<sup>16</sup>

Oxidation of **1** and its isomers to pheomelanin then proceeds via oxidative cyclization of the cysteine side chain to give an *o*-quinonimine intermediate, which undergoes rearrangement

with or without decarboxylation to a series of benzothiazines,<sup>17,18</sup> including 7-(2-amino-2-carboxyethyl)-3-carboxy-5-hydroxy-2*H*-1,4-benzothiazine (**2**) and 7-(2-amino-2-carboxyethyl)-5-hydroxy-3-oxo-3,4-dihydro-2*H*-1,4-benzothiazine (**3**).<sup>19</sup> Further oxidation leads to 2,2'-bi[7-(2-amino-2-carboxyethyl)-3-carboxy-5-hydroxy-2*H*-1,4-benzothiazine] (**4**) as a mixture of diastereoisomers. Oxidation of such dimers affords trichochrome C, which has been isolated together with other structurally related dimers, collectively termed trichochromes, from pheomelanin tissues.<sup>20</sup> These have been proposed as possible chromophoric components of the natural pigments (Figure 1).<sup>9,21,22</sup> All these species would take part in pheomelanin buildup.

Beyond this stage, information about the process of pheomelanin synthesis is virtually absent.

Direct investigation of the natural pigments, on the other hand, has been largely based on spectroscopic analysis<sup>9,10</sup> coupled with chemical degradation studies.<sup>23–27</sup> All these studies supported the notion that pheomelanins consist of benzothiazine and benzothiazole units at various oxidative levels and linked through different bonds.<sup>5,28</sup>

A crucial, so far unsettled, structural issue relates to the identification several decades ago of a series of pyridine carboxylic acids, including pyridine-2,3,4,6-tetracarboxylic acid and 2-(4,5-dicarboxythiazol-2-yl)-3,4,6-pyridine tricarboxylic acid (TPCA), by oxidative degradation of pigments from red chicken feathers.<sup>1,29</sup>

The structure of these fragments led the authors to postulate the presence of (benzo)thiazole-linked isoquinolines of type *I* in natural pheomelanins,<sup>29</sup> which may give rise to TPCA by a

Received: October 15, 2010

Published: February 22, 2011

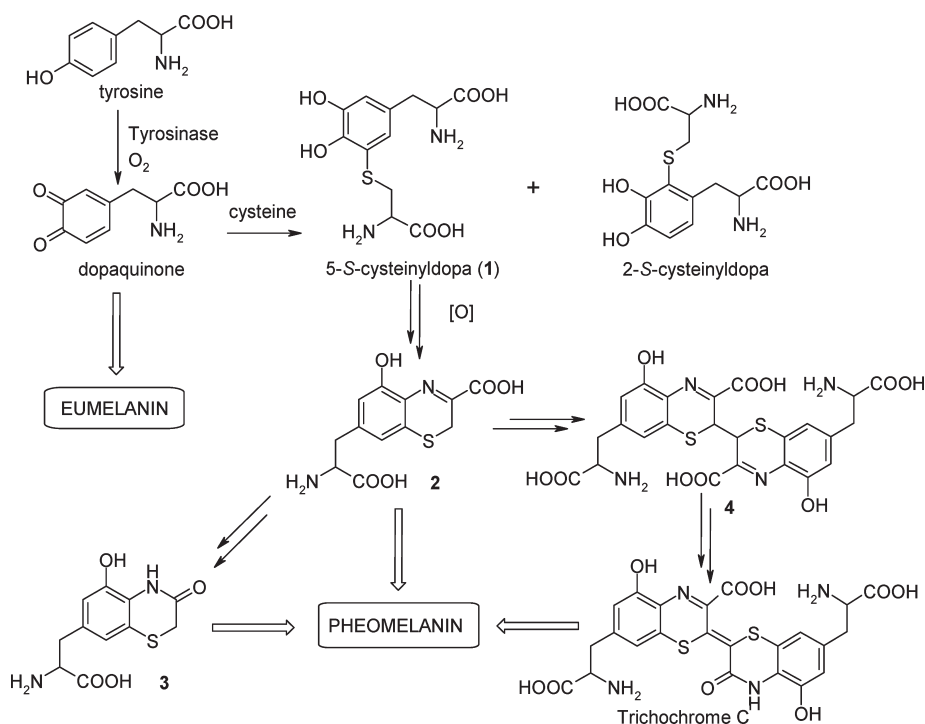


**Figure 1.** Formation of cysteinyl dopas by a deviation of the eumelanin pathway and their oxidation to pheomelanin.

muconic-type oxidative fission as shown in Figure 2.<sup>30</sup> This hypothesis remains unverified. Pyridine units could never be demonstrated in human pheomelanin nor in synthetic pigments, the origin of the main pyridine-containing degradation products remained uncharted, and isoquinoline derivatives have never been isolated in model biomimetic studies of pheomelanin synthesis.<sup>5</sup>

In this paper we report new experimental data that fill most of these gaps. Described herein is the first demonstration in a pheomelanogenesis model of the generation of a dihydroisoquinoline derivative featuring a remarkable dimeric skeleton. The compound afforded TPCA on chemical degradation and exhibited absorption characteristics similar to those of red hair pheomelanin.

## RESULTS AND DISCUSSION

**Identification of a Pyridine Marker from Human Red Hair Pheomelanin.** An initial series of experiments was directed to gauge the presence of isoquinoline-containing constituents in human red hair pheomelanin by chemical degradation. To this end, it seemed of interest to revisit the alkaline  $\text{KMnO}_4$  oxidation method successfully applied in the early studies to the characterization of pigments from red chicken feathers.<sup>31</sup> HPLC analysis of the red hair degradation mixture revealed the presence of a major species that was also generated by degradation of a set of synthetic pheomelanins prepared under different conditions. No detectable amount of the product, however, was present in the degradation mixtures from black hair eumelanin, indicating that it derived from an important and specific pheomelanin component. Accordingly, a procedure was set up that allowed the isolation of the main degradation product in sufficient amounts for structural characterization. For this purpose, the pheomelanin obtained by oxidation of 1 with peroxidase/ $\text{H}_2\text{O}_2$  in the presence

of  $\text{Zn}^{2+}$  was selected because of the higher formation yields of the product relative to other synthetic pigments. Treatment of a 120 mg sample of the synthetic pheomelanin with alkaline  $\text{KMnO}_4$  yielded a complex degradation mixture from which the target product could eventually be isolated in small amounts by preparative HPLC. The compound displayed a pseudomolecular ion peak (ESI(-)/MS) at  $m/z$  381 (HR/MS 380.9672 calcd for  $\text{C}_{13}\text{H}_5\text{N}_2\text{O}_{10}\text{S}$  380.9670) and an absorption maximum at 292 and 318 nm. The  $^1\text{H}$  NMR spectrum was remarkably simple, exhibiting a single resonance (singlet) at  $\delta$  8.56. On this basis, the product was unambiguously formulated as TPCA.<sup>29</sup> The availability of an authentic standard allowed us to secure the identity of the component observed in the degradation mixtures of natural pheomelanins by spiking experiments and LC/MS analysis. This result showed that human red hair pheomelanin contains (benzo)thiazole-linked isoquinoline units akin to those found in gallopheomelanin and giving, on degradation, the structurally significant TPCA (Figure 2).

**Biomimetic Oxidation of 1 and Isolation of Isoquinoline Products.** Information about the nature of the TPCA precursor units was sought through investigation of the oxidation of 1 with peroxidase/ $\text{H}_2\text{O}_2$  in the presence of  $\text{Zn}^{2+}$ . As shown above, this reaction led to a synthetic pigment that provided the richest source of TPCA on degradation. The role of  $\text{Zn}^{2+}$  ions is to slow down the kinetics of pheomelanin synthesis, favoring the accumulation of benzothiazine intermediates.<sup>9,20</sup> Such an effect has also been confirmed in studies on catechol models of 1.<sup>32</sup> Besides being chemically convenient for intermediate isolation and characterization, the addition of  $\text{Zn}^{2+}$  is also of biological relevance since relatively high levels of zinc are found in normal human skin and are known to accumulate in red hair.<sup>10</sup> HPLC analysis coupled with ESI(+)-MS (Figure S1) showed in the early stages of the reaction the generation of two main products, identified as 2 and 3. While 3 accumulated with time and

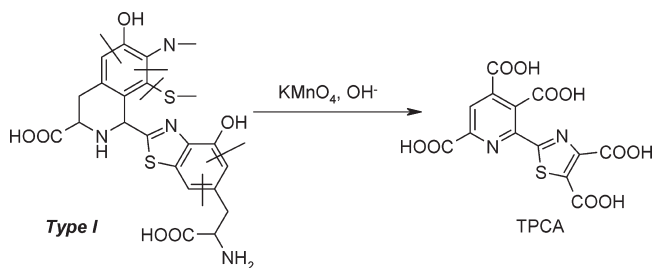
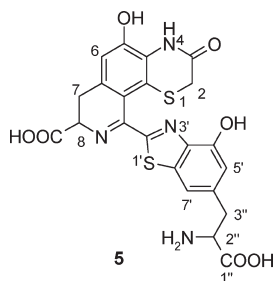


**Figure 2.** Proposed structural units of natural pheomelanins<sup>29</sup> and possible origin of the degradation product TPCA. Lines indicate the bonds involved in fission.

**Table 1.** <sup>1</sup>H NMR (D<sub>2</sub>O/DCI 400 MHz) Data of **5**



position <sup>a</sup>	$\delta_{\text{H}}$ , multiplicity (J, Hz)
2	3.18, s
6	7.05, s
7	3.60, dd (6.0, 14.4) 3.64, dd (6.0, 14.4)
8	5.09, t (6.0)
5' <sup>b</sup>	7.09, s
7' <sup>b</sup>	7.65, s
2''	4.73, t (6.8)
3''	3.39, dd (6.8, 14.8) 3.50, dd (6.8, 14.8)

<sup>a</sup> Assignments based on HMBC correlation. <sup>b</sup> Interchangeable.

remained largely unchanged in the mixture, **2** attained its maximum concentration after about 1 h and then gradually decayed, being replaced by a complex pattern of products including dimers **4** and two additional species, eluting at around 40 and 60 min (HPLC, Figure S1) and exhibiting a pseudomolecular ion peak  $[M + H]^+$  in common at  $m/z$  515.0, suggesting isomeric dimers of **1**.

To gain insight into the structure of these products, the oxidation of **1** was repeated under similar conditions but on a larger scale. When the formation yield of the  $t_{\text{R}}$  40 and 60 min products was maximum (ca. 5 h), the mixture was acidified to pH 2 (care being taken to avoid artifactual side reactions), and the products that precipitated were collected by centrifugation and eventually purified by preparative HPLC. The  $t_{\text{R}}$  40 min product, the most abundant ( $\lambda_{\text{max}}$  248, 282, 346, 392 nm), was obtained as an oil poorly soluble in water and markedly unstable to acids. It displayed three singlets in the aromatic region of the <sup>1</sup>H NMR spectrum (Table 1) at  $\delta$  7.05, 7.09, and 7.65, the latter two exhibiting a distinct cross-peak in the <sup>1</sup>H, <sup>1</sup>H COSY spectrum and correlation with carbons at  $\delta$  143.8 and  $\delta$  37.5 in the HMBC spectrum. In addition, the aliphatic region displayed a two-proton singlet at  $\delta$  3.18 (HMBC correlations with

**Table 2.** NMR Data (400 MHz, methanol-*d*<sub>4</sub>) of **6**

position	$\delta_{\text{H}}$ , multiplicity	$\delta_{\text{C}}$ <sup>a</sup>
2	3.06, s	31.1
6	7.36, s	108.3
7	8.51, s	124.8
5' <sup>b</sup>	6.93, s	113.6
7' <sup>b</sup>	7.50, s	114.3
2''	4.29, m	55.1
3''	3.24, m, 3.44, m	37.6

<sup>a</sup> Assignments based on <sup>1</sup>H, <sup>13</sup>C DEPT HSQC spectrum.

<sup>b</sup> Interchangeable.

carbons at  $\delta$  169.1 and 130.1) and two sets of resonances ( $\delta$  3.39, 3.50, and 4.73 and  $\delta$  3.60, 3.64, and 5.09) whose spin systems and chemical shift values were strongly suggestive of two alanyl side chains, in the second of which the CH proton was unusually downfield shifted, while in the first one the CH proton showed HMBC correlation with the carbon at  $\delta$  37.5. These features were tentatively assigned to a dihydroisoquinoline system linked to a benzothiazole unit as in structure **5**. The  $t_{\text{R}}$  60 min product ( $\lambda_{\text{max}}$  245, 330, 394 nm) proved highly unstable and could not be further characterized.

However, the unfavorable properties of both products prevented a more in-depth spectral analysis, including <sup>13</sup>C NMR spectra, despite several efforts. While sitting in a mildly acidic medium, both the  $t_{\text{R}}$  40 min and  $t_{\text{R}}$  60 min products were converted into species featuring a pseudomolecular ion peak  $[M + H]^+$  at  $m/z$  513.0, suggesting an oxidation step (Figure S2). Moreover, whereas either product could be reduced by treatment with NaBH<sub>4</sub> ( $[M + H]^+$ ,  $m/z$  517.0) (Figure S3), their oxidized forms were relatively more stable. Accordingly, a convenient protocol for structural characterization of the oxidized species was developed, which involved isolation of the  $t_{\text{R}}$  40 min and  $t_{\text{R}}$  60 min products in pure form by preparative HPLC followed by quantitative conversion to the oxidized forms by air exposure in MeOH/HOAc (99:1 v/v). The <sup>1</sup>H NMR spectra of the oxidized  $t_{\text{R}}$  40 min product featured four aromatic singlets (at  $\delta$  6.93, 7.36, 7.50, and 8.51, showing one-bond correlation with carbons at  $\delta$  113.6, 108.3, 114.3, and 124.8) and the lack of one of the alanyl chains, suggesting formation of an isoquinoline ring system. The features of the benzothiazolylalanyl moiety (HMBC correlation between the proton at  $\delta$  6.93 and the CH<sub>2</sub>CH carbon at  $\delta$  37.6 and between the proton at  $\delta$  7.50 and C-3' at  $\delta$  143.7) and of the 3-oxo-1,4-thiazine system (a two-proton signal at  $\delta$  3.06 showing one-bond correlation with a carbon at  $\delta$  31.1 and HMBC correlation with a carbonyl carbon at  $\delta$  168.6) seemed largely unchanged (Table 2).

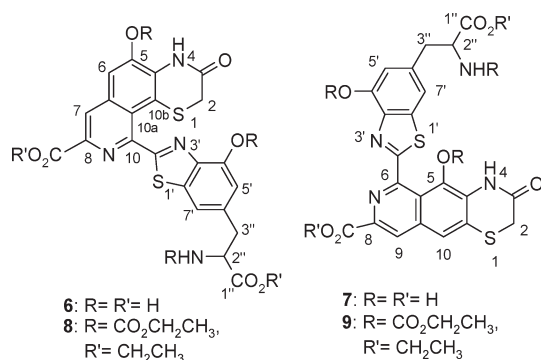
Quite similar features were apparent in the NMR spectra of the oxidized form of the  $t_{\text{R}}$  60 min product including the isoquinoline moiety ( $\delta$  7.09 and 7.83 singlets showing one-bond correlation with carbons at  $\delta$  116.6 and 125.8, respectively), the resonances of the benzothiazolylalanyl unit (one-proton signals at  $\delta$  6.79 and 7.24 linked to carbons at  $\delta$  112.5 and 112.8, respectively, and the  $\delta$  3.37/3.22 (36.1) and 4.35 (53.8) CH<sub>2</sub>CH— system), and the 3-oxothiazine moiety (two-proton singlet at  $\delta$  3.57 linked to a carbon at  $\delta$  28.5) (Table 3). Collectively, these data suggested two isomeric isoquinoline structures, **6** and **7**. However, these compounds proved to be unstable, which prevented further characterization, and eventually a derivatization procedure was deemed necessary for a complete structural analysis. After several trials it

was found that reaction of the products with ethyl chloroformate in ethanol/pyridine<sup>33</sup> by an optimized procedure was the most useful strategy for converting **6** and **7** into stable derivatives fairly soluble in organic solvents. The latter compounds were purified and subjected to extensive spectral analysis.

The product obtained by oxidation and derivatization of the  $t_R$  40 min component exhibited a pseudomolecular ion peak  $[M + Na]^+$  at  $m/z$  807 (HR-ESI (+)/MS found 807.1629 calcd for  $C_{35}H_{36}N_4O_{13}S_2Na$  807.1613), indicating a pentasubstituted derivative. Noticeable features of the  $^1H$  NMR spectrum were (a) a one-proton singlet resonating at  $\delta$  8.54 and showing a one-bond correlation with a carbon signal at  $\delta$  125.1 and a ROESY association with a singlet at  $\delta$  7.98, correlating in turn with a carbon at  $\delta$  117.1, and (b) two one-proton singlets at  $\delta$  7.19 and 7.71, showing cross-peaks in the HSQC spectrum with carbon resonances at  $\delta$  120.7 and 120.2, respectively. Scrutiny of the 2D NMR spectra of the compound, comparison of the data with those of **3** following analogous derivatization with ethyl chloroformate, and, in particular, consideration of the HMBC correlation between the  $\delta$  7.98 proton and the carbon at  $\delta$  141.8 eventually led to formulation of the structure as the *N,O*-ethoxycarbonyl-ethyl ester of 10-[6-(2-amino-2-carboxyethyl)-4-hydroxybenzothiazol-2-yl]-8-carboxy-5-hydroxy-3-oxo-3,4-dihydro-2*H*-[1,4]thiazino[5,6-*h*]isoquinoline (**8**). NMR spectroscopic data for **8** are listed in Table 4.

The product obtained from oxidation and derivatization of the  $t_R$  60 min product displayed the expected pseudomolecular ion peak  $[M + Na]^+$  at  $m/z$  807 (HR-ESI(+)/MS found 807.1629, calcd for  $C_{35}H_{36}N_4O_{13}S_2Na$  807.1613) for a pentasubstituted derivative. Also the NMR spectra (Table S1) were similar to that of the  $t_R$  40 min product following oxidation and derivatization, allowing straightforward identification of the compound as the isomeric *N,O*-ethoxycarbonyl-ethyl ester of 6-[6-(2-amino-2-carboxyethyl)-4-hydroxybenzothiazol-2-yl]-8-carboxy-5-hydroxy-3-oxo-3,4-dihydro-2*H*-[1,4]thiazino[6,5-*g*]isoquinoline (**9**).

Notably in this case two series of signals were observed in the  $^1H$  and  $^{13}C$  NMR spectra with a chemical shift splitting more marked for the resonances of the thiazinoisoquinoline moiety than for those due to the benzothiazole unit. It is possible that this reflects atropisomerism at the benzothiazole–isoquinoline bond due to the steric hindrance of the ethoxycarbonyl group at C-5, as would also be indicated by the lack of signal splitting in the product before derivatization.



**Spectral and Chemical Properties of Dihydroisoquinoline 5.** In view of the lower stability of the  $t_R$  60 min product with respect to **5**, the latter was preferably used.

**Table 3.** NMR Data (400 MHz, methanol-*d*<sub>4</sub>) of **7**

position	$\delta_H$ , multiplicity	$\delta_C^{a,b}$
2	3.57, s	28.5
9	7.89, s	125.8
10 <sup>c</sup>	7.09, s	116.6
5 <sup>c</sup>	6.79, s	112.5
7 <sup>c</sup>	7.24, s	112.8
2''	4.35, bs	53.8
3''	3.22, m, 3.37, m	36.1

<sup>a</sup> Assignments based on  $^1H$ ,  $^{13}C$  DEPT HSQC spectrum. <sup>b</sup> Quaternary carbon resonances:  $\delta$  114.8, 125.2, 127.4, 133.8, 135.1, 137.0 ( $\times 2$ ), 139.5, 140.7, 146.6, 151.3, 165.7, 168.9, 169.7, 171.6. <sup>c</sup> Interchangeable.

**Table 4.** NMR Data (400 MHz, CDCl<sub>3</sub>) of **8**

position	$\delta_H^a$ , multiplicity	$\delta_C^a$
2	3.06, s	30.8
3		166.1
4	8.21, s	
4a		131.3
5		141.8
6	7.98, s	117.1
6a <sup>b</sup>		138.9
7	8.54, s	125.1
8		135.0
CO-C8		164.5
10		150.0
10a		125.1
10b		121.7
2'		170.0
3'a		145.3
4 <sup>b</sup>		144.9
5 <sup>c</sup>	7.19, s	120.7
6'		135.8
7 <sup>c</sup>	7.71, s	120.2
7 <sup>a,b</sup>		140.3
1''		171.2
2''	5.26, m	54.7
3''	3.30, m	38.5

<sup>a</sup> Resonances of ethoxy and ethoxycarbonyl groups:  $^1H$  NMR:  $\delta$  1.25 (3H  $\times 2$ ), 1.34 (3H), 1.46 (3H), 1.48 (3H), 4.14 (2H), 4.20 (2H), 4.28 (2H), 4.43 (2H), 4.52 (2H);  $^{13}C$  NMR:  $\delta$  14.1 (CH<sub>3</sub>  $\times 3$ ), 14.4 (CH<sub>3</sub>), 14.5 (CH<sub>3</sub>), 61.4 (CH<sub>2</sub>), 61.8 (CH<sub>2</sub>), 62.1 (CH<sub>2</sub>), 65.3 (CH<sub>2</sub>), 66.4 (CH<sub>2</sub>), 151.1 (CO), 153.3 (CO), 155.9 (CO). <sup>b,c</sup> Interchangeable.

The UV spectrum of **5** showed a broad band with shoulders around 310 and 360 nm in neutral buffer and displayed reversible shifts in acidic medium to 290, 340, and 400 nm (Figure S4), reflecting the superimposition of different chromophores. However, the acid-induced band at 400 nm could not be accounted for by either the benzothiazole moiety (ca. 300 nm with a shoulder at 320 nm)<sup>34</sup> or the 3-oxo-2*H*-1,4-benzothiazine system (300 nm) alone. Since the spectrum of **5** lost the feature at 400 nm upon reduction to the corresponding tetrahydroisoquinoline with NaBH<sub>4</sub> (Figure S3), it was argued that the 400 nm band was due to the dihydroisoquinolinethiazinone chromophore.

Interestingly, a similar spectrophotometric behavior was exhibited by red hair pheomelanin, which showed in acids a distinct

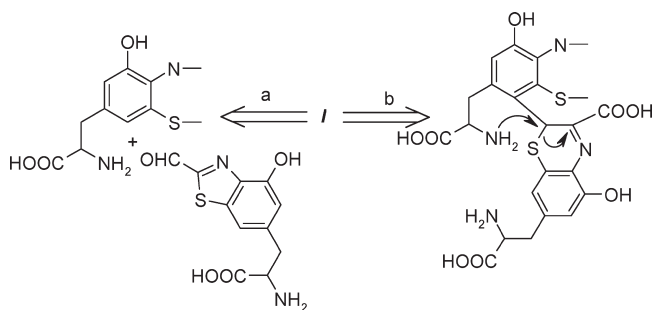


**Figure 3.** Proposed origin of type I tetrahydroisoquinoline units according to Minale et al.<sup>29</sup>

band around 400 nm. Considering that this feature does not match with those of any of the known pheomelanin intermediates, including benzothiazine compounds and the trichochromes,<sup>1,9,21</sup> it could be speculated that the absorption band at 400 nm in the human pheomelanin spectrum is due at least in part to the contribution of structural units related to **5**.

To assess whether and to what extent isoquinoline derivatives are representative of structural components in human red hair pheomelanin, and whether they are precursors to TPCA, further experiments were aimed at determining the chemical degradation behavior of **5**. As expected,  $\text{KMnO}_4$  degradation of **5** led to a significant formation of TPCA in comparison with human pheomelanin and synthetic pigment from dopa and cysteine currently used as a standard pheomelanin,<sup>35</sup> allowing us to conclude that **5** or related units may be the missing precursors of this “orphan” pheomelanin degradation product. A possible artifactual formation of TPCA was ruled out by control experiments in which no trace of the marker was detected from other precursors, including **1**, **3**, or **4**.

**Mechanistic Issues.** The isolation of dihydroisoquinoline derivatives of type **5** raised a number of issues concerning the mechanism of formation of the isoquinoline moiety. In principle, diverse reaction pathways can be envisaged that could lead to the benzothiazole-linked pyridine substructure. For example Minale et al.<sup>29</sup> suggested that TPCA arises from breakdown of partial structure **I** (Figure 2), which features a tetrahydroisoquinoline moiety, and proposed that partial structure **I** is generated via benzothiazine ring contraction, causing C-2 to become exocyclic, thus providing the necessary requisite for isoquinoline ring closure.

The details of the benzothiazole-forming step are unknown and remain one of the unsolved issues in pheomelanin biosynthesis. According to a classical view, benzothiazine ring contraction results in the generation of an aldehyde group, which is then engaged in Pictet–Spengler chemistry with another benzothiazine intermediate (Figure 3, path a). Alternatively, two benzothiazine precursor units could couple at the 2- and 8-positions and then may undergo a transformation by which the benzothiazole and tetrahydroisoquinoline components are formed simultaneously (Figure 3, path b).<sup>1,29</sup>

Although both options are reasonable, they have never been supported by direct experimental evidence. Moreover, the biomimetic experiments reported in the present study indicated the formation of dihydroisoquinoline compounds, whereas previously suggested mechanisms led to tetrahydroisoquinoline derivatives. Since it is known that oxidation of tetrahydroisoquinoline compounds would not stop at the dihydroisoquinoline stage without further conversion to the fully aromatic derivatives,<sup>36</sup> the origin of this discrepancy was addressed by

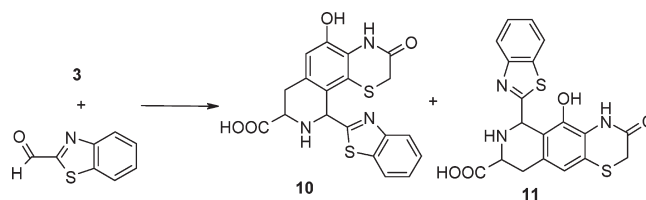


**Figure 4.** Pictet–Spengler reaction of **3** with 2-formylbenzothiazole.

studying the reaction of **3** with commercially available 2-formylbenzothiazole as a model aldehyde compound for Pictet–Spengler chemistry. Under neutral conditions, two main products were formed, which could be isolated and identified as the regioisomeric tetrahydroisoquinoline derivatives **10** and **11** (Figure 4). In the case of **11** the two diastereoisomers **11a/b** could be isolated as separate products (Figure S5).

Notably, no dihydroisoquinoline or higher oxidation product could be detected. Moreover, attempts to oxidize **10** and **11** by peroxidase/ $\text{H}_2\text{O}_2$  failed, the compounds being remarkably stable. On this basis, it was concluded that dihydroisoquinoline derivatives like **5** are unlikely to arise by oxidation of tetrahydroisoquinoline precursors, as suggested by the previous authors.<sup>29</sup> An alternate process accounting for the generation of dihydroisoquinoline derivatives is shown in Figure 5.

In this representative scheme, which illustrates formation of **5**, initial attack of the enamine tautomer of **2** to the corresponding quinone-imine would generate a dimer intermediate. Oxidation of the latter would lead to a spirocyclic intermediate, which would evolve via a ring contraction to give the dihydroisoquinoline derivative. Formation of the 3-oxobenzothiazine moiety would follow from a water addition–oxidation–decarboxylation sequence occurring during or after the coupling process.

The reaction sequence in Figure 5, though basically similar to the mechanism proposed by the early authors,<sup>1,29</sup> differs in that it envisages an additional oxidation step preceding the intramolecular attack of the amino group to give the spirocyclic intermediate. This oxidation step is pivotal for production of **5** since it not only would facilitate nucleophilic attack by the amino group in the intramolecular cyclization process but would also convincingly explain generation of the isoquinoline system at the dihydro level. Alternative coupling at C-2 and C-6 of the quinone-imine and the related enamine generated by oxidation of **2** would account for the isomeric dihydroisoquinoline precursor to **7**. Besides providing an explanation for dihydroisoquinoline formation, the proposed scheme offers a viable mechanism for the origin of benzothiazole rings during pheomelanin synthesis and may well account for the consistent proportion of benzothiazole units evidenced in natural pheomelanins, particularly red hair and chicken feathers, by degradative analysis.<sup>28</sup> This specific issue was recently addressed,<sup>5</sup> but while the formation of benzothiazole moieties was demonstrated as a late event in the process, the possibility that this process is at least in part the outcome of a benzothiazine-coupling step has been so far overlooked and opens new vistas into the process of pheomelanin synthesis *In vivo*. It may be speculated that similar coupling mechanisms may be extended beyond the dimer level, as previously suggested,<sup>29</sup> thus pointing to dihydroisoquinoline cyclization as a chief benzothiazole-forming mechanism of pigment chain elongation. Moreover the mechanism of coupling of **2** as the enamine tautomer to the corresponding quinone-imine may actually offer a unifying pathway accounting also for the

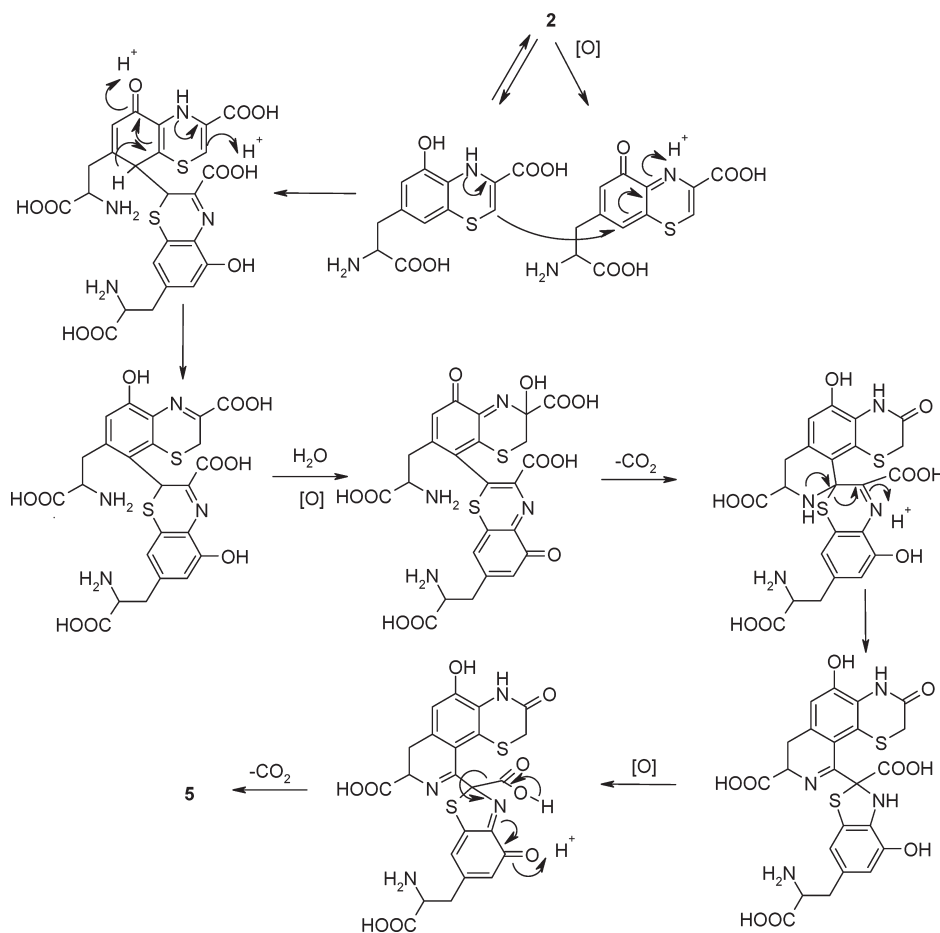


Figure 5. Suggested mechanism of formation of 5.

formation of dimers  $4^{20}$  and, on further oxidation of trichochromes, significant components of pheomelanin tissues.

## CONCLUSIONS

In this paper we provide a contribution to the understanding of the structure and origin of pheomelanins by disclosing isoquinoline subunits in human pheomelanin and the postulated isoquinoline formation pathway in cysteinyl-dopa oxidation. More specifically, we reported (a) the isolation of unprecedented dihydroisoquinoline-containing products from the biomimetic oxidation of 5-*S*-cysteinyl-dopa and a new mechanism for benzothiazole formation via benzothiazine ring contraction in the pigment pathway; (b) the identification of isoquinoline-derived pyridine fragments by oxidative degradation of human red hair pheomelanin; and (c) the close similarity of pheomelanin absorption features to those of the novel dihydroisoquinoline substructures.

As a rule, caution should be exercised in deriving insights from model reactions to account for the behavior of natural systems. Furthermore, the complexity of melanin chemistry raises concern about comparing data from different experimental methodologies. However, the results of the present study clearly show that the diversity of structural motifs emerging from the model synthetic studies provides a solid basis to interpret the chemical and photobiological properties of natural pigments, supporting the value of the integrated approach described in this study as a

unique investigative tool. Elucidation of the role of isoquinoline substructures in the absorption and emission spectra of human pheomelanin is a main focus of future research aimed to unravel the pigment-mediated mechanisms of generation of dermatitic or carcinogenic photoproducts supposedly implicated in the UV susceptibility trait.

## EXPERIMENTAL SECTION

**General Experimental Procedures.** ICR-FT ESI(+ or -)/MS were obtained in MeOH and ESI(+)/MS spectra were obtained in 1% HCO<sub>2</sub>H/MeOH. UV-vis spectra were obtained on a diode array spectrophotometer equipped with a thermostated sample cell holder. <sup>1</sup>H NMR spectra were recorded at 400 or 600 MHz; <sup>13</sup>C NMR spectra at 100 MHz. <sup>1</sup>H, <sup>13</sup>C (DEPT) HSQC, and <sup>1</sup>H, <sup>13</sup>C HMBC experiments were run at 400 or 600 MHz, on instruments equipped with a 5 mm <sup>1</sup>H/broadband gradient probe with inverse geometry using standard pulse programs. The HMBC experiments used a 100 ms long-range coupling delay. Chemical shifts are reported in  $\delta$  values (ppm) downfield from TMS. Analytical HPLC was carried out on an apparatus equipped with a UV detector set at 254, 280, or 340 nm or ESI/MS using a Spherclone ODS (5  $\mu$ m, 4.6  $\times$  250 mm) column. Gradient A (0.5% TFA (eluant a)/MeOH (eluant b): from 10 to 15% b, 0–15 min; from 15 to 60% b, 15–55 min; 60% b, 55–65 min; from 60 to 80% b, 65–80 min; 80% b, 80–90 min) or gradient B (H<sub>2</sub>O (eluant a)/MeCN (eluant b): 5% b, 0–5 min; from 5 to 90% b, 5–40 min) was used, at a flow rate of 0.8 mL/min. Semipreparative HPLC was carried out on an instrument coupled with a UV detector set at 254 or 280 nm using an Econosil C18 (10  $\mu$ m, 10  $\times$  250 mm) column.

Gradient A or gradient B was used, at flow rates, respectively, of 3 or 3.5 mL/min. Preparative HPLC was carried out on an instrument coupled with a UV detector set at 254 or 280 nm using an Econosil C18 (10  $\mu$ m, 22  $\times$  250 mm). Gradient A or eluant C (0.3% TFA/MeOH, 35/65 v/v) was used, at a flow rate of 20 or 9 mL/min, respectively. Purity of isolated compounds was estimated by  $^1$ H NMR analysis.

L-Dopa, L-cysteine, H<sub>2</sub>O<sub>2</sub> (30% v/v), ZnSO<sub>4</sub>·7H<sub>2</sub>O, KMnO<sub>4</sub>, Na<sub>2</sub>S<sub>2</sub>O<sub>5</sub>, NaBH<sub>4</sub>, ethyl chloroformate, benzothiazole-2-carboxaldehyde, horseradish peroxidase (EC 1.11.1.7), and mushroom tyrosinase (EC 1.14.18.1) were commercially available and were used as obtained. 5-S-Cysteinyl-dopa (**1**),<sup>37</sup> 7-(2-amino-2-carboxyethyl)-5-hydroxy-3-oxo-3,4-dihydro-2H-1,4-benzothiazine (**3**),<sup>38</sup> 7-(2-amino-2-carboxyethyl)-3-carboxy-5-hydroxy-3,4-dihydro-2H-1,4-benzothiazine (reduced **2**),<sup>39</sup> and 2,2'-bi[7-(2-amino-2-carboxyethyl)-3-carboxy-5-hydroxy-2H-1,4-benzothiazine] (**4**)<sup>20</sup> were prepared as described. Pheomelanin from L-dopa and L-cysteine was prepared by tyrosinase/O<sub>2</sub> oxidation as reported.<sup>35</sup> Pheomelanins from **1** by peroxidase/H<sub>2</sub>O<sub>2</sub> oxidation were prepared as reported, with slight modifications.<sup>9,14</sup> Red and black hair were collected from healthy volunteers. Only hair samples that had not received dyeing or other chemical treatments were included in this study.

**Alkaline Permanganate Degradation.** The appropriate sample (viz., synthetic pheomelanins, compounds **1**, **3**, **4**, **5**) (5 mg) was dissolved in 2 M Na<sub>2</sub>CO<sub>3</sub> (200  $\mu$ L). Red or black human hair (5 mg) was homogenized in 2 M Na<sub>2</sub>CO<sub>3</sub> (200  $\mu$ L) in a glass-glass potter. The mixture thus obtained was treated with a 3% solution of KMnO<sub>4</sub> (1 mL), added in 10 portions at 10 min intervals. Na<sub>2</sub>S<sub>2</sub>O<sub>5</sub> (72 mg) was then added to destroy residual oxidant, and the mixture was filtered through nylon membranes (13 mm, 0.45  $\mu$ m; Alltech Associates, Deerfield, IL, USA) and washed with H<sub>2</sub>O (2  $\times$  2 mL). The filtrate was acidified to pH 1, concentrated to a final volume of 200  $\mu$ L, and analyzed by HPLC/UV (gradient A, detection at 254 nm).

**Isolation of 2-(4,5-Dicarboxythiazol-2-yl)-3,4,6-pyridine-tricarboxylic Acid (TPCA).** Pheomelanin (120 mg), obtained by oxidation of **1** (250 mg, 0.79 mmol) with 50 units/mL of peroxidase and 285  $\mu$ L of 30% v/v H<sub>2</sub>O<sub>2</sub> in the presence of ZnSO<sub>4</sub>·7H<sub>2</sub>O (273 mg, 1.2 molar equiv),<sup>9,14</sup> was dissolved in 2 M Na<sub>2</sub>CO<sub>3</sub> (4.8 mL) and oxidized with a 3% aqueous solution of KMnO<sub>4</sub> (16 mL), added in 10 portions at 10 min intervals. The mixture was treated with Na<sub>2</sub>S<sub>2</sub>O<sub>5</sub> (1.15 g) to destroy residual oxidant, filtered through nylon membranes (47 mm, 0.45  $\mu$ m; Alltech Associates, Deerfield, IL, USA), and washed with H<sub>2</sub>O (2  $\times$  50 mL). The supernatant was acidified to pH 1, concentrated to a final volume of 20 mL, and extracted with EtOAc (6  $\times$  30 mL). The organic layer was taken to dryness, dissolved in 0.1 M HCl (1 mL), and purified by semipreparative HPLC (gradient A, detection at 254 nm) to give TPCA<sup>29</sup> (yellowish oil, *t*<sub>R</sub> 35.8 min, 2 mg, purity >95%): UV (MeOH)  $\lambda_{\text{max}}$  292, 318 nm; HR-ESI(-)/MS found *m/z* 380.9672 ([M - H]<sup>-</sup>), calcd for C<sub>13</sub>H<sub>5</sub>N<sub>2</sub>O<sub>10</sub>S *m/z* 380.9670;  $^1$ H NMR (D<sub>2</sub>O/DCl, 500 MHz) 8.56 (s).

**Oxidation of 1.** To a solution of **1** (12 mM) in 0.1 M phosphate buffer (pH 6.8; 150 mL) were added ZnSO<sub>4</sub>·7H<sub>2</sub>O (1.2 molar equiv), horseradish peroxidase (50 units/mL final concentration), and 30% v/v H<sub>2</sub>O<sub>2</sub> up to a 38 mM final concentration. The mixture was allowed to sit at room temperature under vigorous stirring for 24 h. Aliquots of the reaction mixture were periodically withdrawn, reduced with NaBH<sub>4</sub> when required, and analyzed by HPLC (gradient A, detection at 280 or 340 nm). For preparative purposes the reaction was carried out on 500 mg of **1**, and after 5 h the mixture was acidified to pH 2, the solid was collected by centrifugation (6793g  $\times$  min, 4 °C, 30 min), and purified by preparative HPLC (gradient A, detection at 280 nm) to afford the product eluting at *t*<sub>R</sub> 39.8 min (orange-brown oil, 20 mg, 3% yield, purity >95%; identified as 10-[6-(2-amino-2-carboxyethyl)-4-hydroxybenzothiazol-2-yl]-8-carboxy-5-hydroxy-3-oxo-3,4,7,8-tetrahydro-2H-[1,4]thiazino[5,6-*h*]isoquinoline (**5**); UV (0.1 M HCl)  $\lambda_{\text{max}}$  248, 282, 346, 392 nm; ESI(+)/MS *m/z* 515.0 ([M + H]<sup>+</sup>); for NMR data see

Table 1) and the product eluting at *t*<sub>R</sub> 63.7 min (brown oil, 17 mg, 2% yield, purity >95% HPLC analysis; UV (0.1 M HCl)  $\lambda_{\text{max}}$  245, 330, 394 nm; ESI(+)/MS *m/z* 515.0 [M + H]<sup>+</sup>).

A solution of either the *t*<sub>R</sub> 39.8 min product or the *t*<sub>R</sub> 63.7 min product (15 mg, 0.03 mmol) in 15 mL of MeOH/HOAc (99:1 v/v) was allowed to sit at room temperature under vigorous stirring. Aliquots of the reaction mixture were periodically withdrawn and analyzed by HPLC (gradient A, detection at 340 nm). After 24 h the mixture was taken to dryness to afford, respectively, **6** (brown oil, *t*<sub>R</sub> 50.1 min, 15 mg, 99% yield, purity >95%) or **7** (brown oil, *t*<sub>R</sub> 80.6 min, 15 mg, 99% yield, purity >95%).

**10-[6-(2-Amino-2-carboxyethyl)-4-hydroxybenzothiazol-2-yl]-8-carboxy-5-hydroxy-3-oxo-3,4-dihydro-2H-[1,4]thiazino[5,6-*h*]isoquinoline (**6**):** UV (EtOH)  $\lambda_{\text{max}}$  294, 355, 393 nm; HR-ESI(-)/MS found *m/z* 511.0400 ([M - H]<sup>-</sup>), calcd for C<sub>22</sub>H<sub>15</sub>N<sub>4</sub>O<sub>7</sub>S<sub>2</sub> *m/z* 511.0388; for NMR data see Table 2.

**6-[6-(2-Amino-2-carboxyethyl)-4-hydroxybenzothiazol-2-yl]-8-carboxy-5-hydroxy-3-oxo-3,4-dihydro-2H-[1,4]thiazino[6,5-*g*]isoquinoline (**7**):** UV (EtOH)  $\lambda_{\text{max}}$  273, 318, 397 nm; HR-ESI(-)/MS found *m/z* 511.0410 ([M - H]<sup>-</sup>), calcd for C<sub>22</sub>H<sub>15</sub>N<sub>4</sub>O<sub>7</sub>S<sub>2</sub> *m/z* 511.0388; for NMR data see Table 3.

**Ethyl Chloroformate Derivatization of 3.** The ethyl chloroformate derivatization procedure was performed as reported,<sup>33</sup> with modifications. A solution of **3** (17.5 mg, 0.065 mmol) in 100 mL of H<sub>2</sub>O/EtOH/Py (60:64:16 v/v) was treated with ethyl chloroformate (6 mL), added in 10 portions at 3 min intervals. The mixture was extracted with CHCl<sub>3</sub> (3  $\times$  80 mL), and the combined organic layers were dried over Na<sub>2</sub>SO<sub>4</sub>. The residue was dissolved in EtOH and taken to dryness (4  $\times$  10 mL) to convert the mixed anhydride formed into ethyl esters.<sup>33</sup> The residue was then dissolved in CHCl<sub>3</sub> and washed with 0.01 M HCl (3  $\times$  80 mL) to remove residual pyridine. The final residue was taken up in CHCl<sub>3</sub>/MeCN (1 mL, 1:1 v/v) and purified by semipreparative HPLC (gradient B, detection at 280 nm). The eluate was taken to dryness, and the residue was dissolved in CHCl<sub>3</sub> and dried over Na<sub>2</sub>SO<sub>4</sub> to eventually afford the *N,O*-ethoxycarbonyl-ethyl ester of **3** (yellowish oil, *t*<sub>R</sub> 24.4 min, 6 mg, 20% yield, purity >95%): ESI(+)/MS *m/z* 441.0 [M + H]<sup>+</sup>;  $^1$ H NMR (CDCl<sub>3</sub>, 400 MHz)  $\delta$  1.24 (6H, m, OCH<sub>2</sub>CH<sub>3</sub>); 1.40 (3H, m, OCH<sub>2</sub>CH<sub>3</sub>); 4.12 (2H, q, *J* = 7.2 Hz, OCH<sub>2</sub>CH<sub>3</sub>); 4.19 (2H, q, *J* = 7.2 Hz, OCH<sub>2</sub>CH<sub>3</sub>); 4.33 (2H, q, *J* = 7.2 Hz, OCH<sub>2</sub>CH<sub>3</sub>); 3.41 (2H, s, H-2); 3.06 (2H, m, CH<sub>2</sub>CH); 5.20 (1H, m, CH<sub>2</sub>CH); 6.95 (1H, s, H-6 or H-8), 6.98 (1H, s, H-8 or H-6); 7.87 (1H, s, NH).

**Ethyl Chloroformate Derivatization of 6 and 7.** The ethyl chloroformate derivatization procedure was performed as reported,<sup>33</sup> with modifications. Briefly, a solution of **6** or **7** (10 mg, 0.020 mmol) in 30 mL of H<sub>2</sub>O/EtOH/Py (60:64:16 v/v) was treated with ethyl chloroformate (1.8 mL), added in 10 portions at 3 min intervals. The final residue, obtained after workup as described, was taken up in CHCl<sub>3</sub>/MeCN (1 mL, 1:1 v/v) and purified by semipreparative HPLC (gradient B, detection at 280 nm). The eluate was taken to dryness, and the residue was dissolved in CHCl<sub>3</sub> and dried over Na<sub>2</sub>SO<sub>4</sub> to eventually afford the *N,O*-ethoxycarbonyl-ethyl ester of **6** (**8**, yellow oil, *t*<sub>R</sub> 31.2 min, 5 mg, 30% yield, purity >95%) or of **7** (**9**, yellow oil, *t*<sub>R</sub> 31.6 min, 2 mg, 10% yield, purity >95%).

**8:** UV (EtOH)  $\lambda_{\text{max}}$  294, 350, 385 nm; HR-ESI(+)/MS found *m/z* 807.1629 ([M + Na]<sup>+</sup>), calcd for C<sub>35</sub>H<sub>36</sub>N<sub>4</sub>O<sub>13</sub>S<sub>2</sub>Na *m/z* 807.1613; for NMR data see Table 4.

**9:** UV (EtOH)  $\lambda_{\text{max}}$  294, 341, 394 nm; HR-ESI(+)/MS found *m/z* 807.1630 ([M + Na]<sup>+</sup>), calcd for C<sub>35</sub>H<sub>36</sub>N<sub>4</sub>O<sub>13</sub>S<sub>2</sub>Na *m/z* 807.1613; for NMR data see Table S1.

**Isolation of 10 and 11a/b.** To a solution of **3** (100 mg, 0.37 mmol) in 0.1 M phosphate buffer (pH 7.4; 25 mL) was added a solution of benzothiazole-2-carboxaldehyde (60 mg, 0.37 mmol) in MeCN, and the mixture was allowed to sit at room temperature under vigorous

stirring. After 7 h the reaction mixture was acidified to pH 1 and extracted with EtOAc (10 × 30 mL). The combined organic layers were taken to dryness, and the residue was dissolved in H<sub>2</sub>O/MeOH (2 mL, 1:1 v/v) and purified by preparative HPLC (eluant C, detection at 254 nm). The eluates were concentrated to a final volume of 20 mL and extracted with EtOAc (10 × 30 mL), and the combined organic layers were dried over Na<sub>2</sub>SO<sub>4</sub> to eventually afford **10** (yellow oil, *t*<sub>R</sub> 12.9 min, 7 mg, 4% yield, purity >98%), **11a** (yellow oil, *t*<sub>R</sub> 26.8 min, 6 mg, 4% yield, purity >98%), and **11b** (yellow oil, *t*<sub>R</sub> 39.3 min, 13 mg, 8% yield, purity >98%).

**10-Benzothiazol-2-yl-8-carboxy-5-hydroxy-3-oxo-3,4,7,8,9,10-hexahydro-2H-[1,4]thiazino[5,6-*h*]isoquinoline (10):** UV (EtOH)  $\lambda_{\text{max}}$  236, 269, 299 nm; HR-ESI(-)/MS found *m/z* 412.0432 ([M - H]<sup>-</sup>), calcd for C<sub>19</sub>H<sub>14</sub>N<sub>3</sub>O<sub>4</sub>S<sub>2</sub> *m/z* 412.0431; for NMR data see Table S2.

**6-Benzothiazol-2-yl-8-carboxy-5-hydroxy-3-oxo-3,4,6,7,8,9-hexahydro-2H-[1,4]thiazino[6,5-*g*]isoquinoline (11a/b) (11a):** UV (EtOH)  $\lambda_{\text{max}}$  220, 244, 294 nm; HR-ESI(-)/MS found *m/z* 412.0436 ([M - H]<sup>-</sup>), calcd for C<sub>19</sub>H<sub>14</sub>N<sub>3</sub>O<sub>4</sub>S<sub>2</sub> *m/z* 412.0431; for NMR data see Table S3.

**11b:** UV (EtOH)  $\lambda_{\text{max}}$  220, 243, 294 nm; HR-ESI(-)/MS found *m/z* 412.0436 ([M - H]<sup>-</sup>), calcd for C<sub>19</sub>H<sub>14</sub>N<sub>3</sub>O<sub>4</sub>S<sub>2</sub> *m/z* 412.0431; for NMR data see Table S3.

## ■ ASSOCIATED CONTENT

**S Supporting Information.** NMR data for **9**, **10**, **11a/b**; HPLC elution profile of the oxidation mixture of **1** with peroxidase/H<sub>2</sub>O<sub>2</sub> in the presence of Zn<sup>2+</sup> at different times; HPLC/UV traces and UV-vis spectra of *t*<sub>R</sub> 39.8 min and *t*<sub>R</sub> 63.7 min products and their reduced and oxidized forms; HPLC profile of the reaction mixture of **3** with benzothiazole-2-carboxaldehyde; NMR spectra of **5**, **6**, **7**, *N,O*-ethoxycarbonyl-ethyl ester of **3**, **8**, **9**, **10**, **11a**, **11b**. This material is available free of charge via the Internet at <http://pubs.acs.org>.

## ■ AUTHOR INFORMATION

### Corresponding Author

\*Tel: +39-081-674133. E-mail: alesnapo@unina.it.

## ■ ACKNOWLEDGMENT

M.d.I. acknowledges support from Italian MIUR (PRIN projects). We thank M. Pappini from Centro Interdipartimentale Grandi Apparecchiature (CIGA), University of Milan, for ICR-FTMS experiments.

## ■ REFERENCES

- Thomson, R. H. *Angew. Chem., Int. Ed. Engl.* **1974**, *13*, 305–312.
- Prota, G. *Melanins and Melanogenesis*; Academic Press: San Diego, CA, 1992.
- Di Donato, P.; Napolitano, A. *Pigm. Cell Res.* **2003**, *16*, 532–539.
- Sturm, R. A.; Teasdale, R. D.; Box, N. F. *Gene* **2001**, *277*, 49–62.
- Simon, J. D.; Peles, D.; Wakamatsu, K.; Ito, S. *Pigm. Cell Melanoma Res.* **2009**, *22*, 563–579.
- Simon, J. D.; Peles, D. N. *Acc. Chem. Res.* **2010**, *43*, 1452–1460.
- Takeuchi, S.; Zhang, W.; Wakamatsu, K.; Ito, S.; Hearing, V. J.; Kraemer, K. H.; Brash, D. E. *Proc. Natl. Acad. Sci. U. S. A.* **2004**, *101*, 15076–15081.
- Ye, T.; Pawlak, A.; Sarna, T.; Simon, J. D. *Photochem. Photobiol.* **2008**, *84*, 437–443.
- Napolitano, A.; De Lucia, M.; Panzella, L.; d'Ischia, M. *Photochem. Photobiol.* **2008**, *84*, 593–599.
- Liu, Y.; Hong, L.; Wakamatsu, K.; Ito, S.; Adhyaru, B.; Cheng, C. Y.; Bowers, C. R.; Simon, J. D. *Photochem. Photobiol.* **2005**, *81*, 135–144.
- Simon, J. D.; Hong, L.; Peles, D. N. *J. Phys. Chem. B* **2008**, *112*, 13201–13217.
- Chedekel, M. R.; Smith, S. K.; Post, P. W.; Pokora, A.; Vessell, D. L. *Proc. Natl. Acad. Sci. U. S. A.* **1978**, *75*, 5395–5399.
- Ye, T.; Hong, L.; Garguilo, J.; Pawlak, A.; Edwards, G. S.; Nemanich, R. J.; Sarna, T.; Simon, J. D. *Photochem. Photobiol.* **2006**, *82*, 733–737.
- Panzella, L.; Szweczyk, G.; d'Ischia, M.; Napolitano, A.; Sarna, T. *Photochem. Photobiol.* **2010**, *86*, 757–764.
- Ito, S.; Wakamatsu, K. *Photochem. Photobiol.* **2008**, *103*, 14785–14789.
- Ito, S.; Prota, G. *Experientia* **1977**, *33*, 1118–1119.
- Napolitano, A.; Memoli, S.; Crescenzi, O.; Prota, G. *J. Org. Chem.* **1996**, *61*, 598–604.
- Napolitano, A.; Memoli, S.; Prota, G. *J. Org. Chem.* **1999**, *64*, 3009–3011.
- Crescenzi, S.; Misuraca, G.; Novellino, E.; Prota, G. *Chim. Ind. (Milan, Italy)* **1975**, *57*, 392–393.
- Napolitano, A.; Di Donato, P.; Prota, G. *J. Org. Chem.* **2001**, *66*, 6958–6966.
- Simon, J. D.; Goldsmith, M. R.; Hong, L.; Kempf, V. R.; McGuckin, L. E. L.; Ye, T.; Zuber, G. *Photochem. Photobiol.* **2006**, *82*, 318–323.
- Ye, T.; Lamb, L. E.; Wakamatsu, K.; Ito, S.; Simon, J. D. *Photochem. Photobiol. Sci.* **2003**, *2*, 821–823.
- Wakamatsu, K.; Ito, S.; Rees, J. L. *Pigm. Cell Res.* **2002**, *15*, 225–232.
- Napolitano, A.; Vincenzi, M. R.; Di Donato, P.; Monfrecola, G.; Prota, G. *J. Invest. Dermatol.* **2000**, *114*, 1141–1147.
- Panzella, L.; Manini, P.; Monfrecola, G.; d'Ischia, M.; Napolitano, A. *Pigm. Cell Res.* **2007**, *20*, 128–133.
- Greco, G.; Wakamatsu, K.; Panzella, L.; Ito, S.; Napolitano, A.; d'Ischia, M. *Pigm. Cell Melanoma Res.* **2009**, *22*, 319–327.
- Napolitano, A.; Vincenzi, M. R.; d'Ischia, M.; Prota, G. *Tetrahedron Lett.* **1996**, *37*, 6799–6802.
- Wakamatsu, K.; Ohtara, K.; Ito, S. *Pigm. Cell Melanoma Res.* **2009**, *22*, 474–486.
- Minale, L.; Fattorusso, E.; Cimino, G.; De Stefano, S.; Nicolaus, R. A. *Gazz. Chim. Ital.* **1969**, *99*, 431–449.
- Sawaki, Y.; Foote, C. S. *J. Am. Chem. Soc.* **1983**, *105*, 5035–5040.
- Fattorusso, E.; Minale, L.; Cimino, G.; De Stefano, S.; Nicolaus, R. A. *Gazz. Chim. Ital.* **1969**, *99*, 29–45.
- Tesema, T. J.; Pham, D. M.; Franz, K. J. *Inorg. Chem.* **2008**, *47*, 1087–1095.
- Husek, P. *FEBS Lett.* **1991**, *280*, 354–356.
- Nezirevic Dernroth, D.; Arstrand, K.; Greco, G.; Panzella, L.; Napolitano, A.; Kagedal, B. *Clin. Chim. Acta* **2010**, *411*, 1195–1203.
- Ito, S. *Pigm. Cell Res.* **1989**, *2*, 53–56.
- Bobbitt, J. M. In *Heterocyclic Chemistry*; Katritzky, A. R., Boulton, A. J., Eds.; Academic Press: New York, 1973; Vol. 15, p 117.
- Chioccare, F.; Novellino, E. *Synth. Commun.* **1986**, *16*, 967–969.
- Prota, G.; Scherillo, G.; Nicolaus, R. A. *Gazz. Chim. Ital.* **1968**, *98*, 495–510.
- Prota, G.; Crescenzi, S.; Misuraca, G.; Nicolaus, R. A. *Experientia* **1970**, *26*, 1508–1509.